

Marone

b Values and $\omega^{-\gamma}$ Seismic Source Models: Implications for Tectonic Stress Variations Along Active Crustal Fault Zones and the Estimation of High-Frequency Strong Ground Motion

THOMAS C. HANKS

U.S. Geological Survey, Menlo Park, California 94025

In this study the tectonic stress along active crustal fault zones is taken to be of the form $\bar{\sigma}(y) + \Delta\sigma_p(x, y)$, where $\bar{\sigma}(y)$ is the average tectonic stress at depth y and $\Delta\sigma_p(x, y)$ is a seismologically observable, essentially random function of both fault plane coordinates; the stress differences arising in the course of crustal faulting are derived from $\Delta\sigma_p(x, y)$. Empirically known frequency of occurrence statistics, moment-magnitude relationships, and the constancy of earthquake stress drops may be used to infer that the number of earthquakes N of dimension $\geq r$ is of the form $N \sim 1/r^2$ and that the spectral composition of $\Delta\sigma_p(x, y)$ is of the form $|\Delta\tilde{\sigma}_p(k)| \sim 1/k^2$, where $\Delta\tilde{\sigma}_p(k)$ is the two-dimensional Fourier transform of $\Delta\sigma_p(x, y)$ expressed in radial wave number k . The $\gamma = 2$ model of the far-field shear wave displacement spectrum is consistent with the spectral composition $|\Delta\tilde{\sigma}_p(k)| \sim 1/k^2$, provided that the number of contributions to the spectral representation of the radiated field at frequency f goes as $(k/k_0)^2$, consistent with the quasi-static frequency of occurrence relation $N \sim 1/r^2$; k_0 is a reference wave number associated with the reciprocal source dimension. Separately, a variety of seismologic observations suggests that the $\gamma = 2$ model is the one generally, although certainly not always, applicable to the high-frequency spectral decay of the far-field radiation of earthquakes. In this framework, then, b values near 1, the general validity of the $\gamma = 2$ model, and the constancy of earthquake stress drops independent of size are all related to the average spectral composition of $\Delta\sigma_p(x, y)$, $|\Delta\tilde{\sigma}_p(k)| \sim 1/k^2$. Should one of these change as a result of premonitory effects leading to failure, as has been specifically proposed for b values, it seems likely that one or all of the other characteristics will change as well from their normative values. Irrespective of these associations, the far-field, high-frequency shear radiation for the $\gamma = 2$ model in the presence of anelastic attenuation may be interpreted as band-limited, finite duration white noise in acceleration. Its rms value, a_{rms} , is given by the expression $a_{rms} = 0.85[2^{1/2}(2\pi)^2/106](\Delta\sigma/\rho R)(f_{max}/f_0)^{1/2}$, where $\Delta\sigma$ is the earthquake stress drop, ρ is density, R is hypocentral distance, f_0 is the spectral corner frequency, and f_{max} is determined by R and specific attenuation $1/Q$. For several reasons, one of which is that it may be estimated in the absence of empirically defined ground motion correlations, a_{rms} holds considerable promise as a measure of high-frequency strong ground motion for engineering purposes.

INTRODUCTION

Very little is known about the heterogeneities in material properties and tectonic stress that exist along active crustal fault zones, yet such heterogeneities are likely to play a central role in earthquake mechanics. It is now known that crustal earthquake stress drops, in their average value $\Delta\sigma$, are several tens of bars and that this value is independent of source strength over 12 orders of magnitude in seismic moment [e.g., Aki, 1972; Thatcher and Hanks, 1973; Kanamori and Anderson, 1975; Hanks, 1977]. Because earthquakes are generally episodic functions of space and time along even the most well developed crustal fault zones, it may then be inferred that stress variations of at least $\Delta\sigma$ commonly exist along active crustal fault zones (although they might be greatly reduced, if not eliminated, at the time and place of throughgoing earthquake faulting, giving rise, for example, to the notably aseismic section of the San Andreas fault that broke in the great earthquake of 1857). But because it may also be inferred that such faults, in general, can be no further away from repeated failure than stress reaccumulation comparable to $\Delta\sigma$, it seems plain that tectonic stress heterogeneities of the order of $\Delta\sigma$ must play a central role in determining why a particular earthquake occurs at a particular point in space and time and therefore in any rational capability that purports to predict earthquakes.

Beyond these truisms, analysis of the nature and extent of stress heterogeneities along seismically active faults is complicated by important but poorly understood problems. One of

these is the average tectonic stress operative to cause failure on the fault zone in the first place; whether this value is of the order of 100 bars (or perhaps somewhat less) or of the order of a kilobar (or perhaps somewhat greater) is as yet unresolved [e.g., Hanks, 1977]. In the first case one may anticipate that variations in tectonic stress must be of the order of 100% of the average value, but in the second case they need only be a small fraction of the average value (although they could be larger).

A second difficulty is that variations in the stresses driving relative motions, in the self-stress [Andrews, 1978] resulting from past faulting episodes (which may be quite nonuniform if nonuniform faulting displacements are common in the case of individual earthquakes), and in material properties along the fault zone all contribute to inhomogeneity in tectonic stresses along the fault zone of interest. Even if the amplitude-wavelength content of actual stress variations along faults was known, which it is not, a difficult problem would remain in separating out the causative processes to which it should be related.

Similarly, there is accumulating evidence that the dynamic faulting displacements and associated stress differences can be highly inhomogeneous in the course of crustal faulting, and it is natural to suspect (but difficult to prove) that these inhomogeneities arise from variations of the preexisting tectonic stresses across the incipient rupture surface. For both the San Fernando (for example, Hanks [1974] and Bouchon [1978]), among many such investigations) and the Borrego Mountain [Burdick and Mellman, 1976; Heaton and Helmberger, 1977] earthquakes, there is considerable evidence that faulting was initiated with localized but massive faulting with associated stress differences not at all representative of those inferred for the entire faulting process. In a similar manner the larger peak

accelerations ($\geq 0.1g$) at close distances ($R \approx 10$ km) almost certainly represent localized, dynamic stress differences many times greater than the average earthquake stress drop [Hanks and Johnson, 1976]. In a very real sense, of course, the ideas presented in the studies cited above are simply scaled-down versions (in spatial dimension and wave period) of the complex, multiple-event interpretation of large and great earthquakes (a number of such investigations are referenced by Das and Aki [1977], who present their barrier model of the earthquake mechanism partially in this context).

In any event, considerable interest has developed around these observations and ideas, for at least two important reasons. First, higher-quality recordings and more detailed analysis of such earthquakes may provide a clearer understanding of the nature and extent of tectonic stress heterogeneities along active crustal fault zones. Second, reliable estimates of high-frequency strong ground motion and their use in the aseismic design of high-frequency structures depend quite strongly on the nature and extent of these localized dynamic stress differences that develop in the course of crustal faulting.

In this study the problem of tectonic stress variations is addressed through interpretations, developed herein, of b -value data and the high-frequency spectral characteristics of the radiated field (ω^{-7} models) for crustal earthquakes. In fact, however, the quantities being investigated are stress differences available to be released at the time of faulting, to which may be added a stress function of which even the average value is unspecified in this study and which, in the absence of additional information, is unknown. Following the ideas of Andrews [1978], one may infer but cannot prove that this unknown stress function is intrinsically smooth, arising fundamentally from large-scale stresses driving relative motion across the fault, and that the actual variations in tectonic stresses along active crustal fault zones are, to a first approximation, reasonably estimated through the ideas developed in this study.

b VALUES AND EARTHQUAKE STRESS DROPS

Hanks [1977] showed that the relations between frequency of occurrence N of earthquakes of magnitude $\geq M$,

$$\log N = a - bM \quad (1)$$

between seismic moment M_0 and M ,

$$\log M_0 = cM + d \quad (2)$$

and between source radius r , earthquake stress drop $\Delta\sigma$, and M_0 ,

$$M_0 = k\Delta\sigma r^3 \quad (3)$$

can be combined to obtain, using $b = 1$ and $c = 1.5$,

$$N = \text{const}/(\overline{\Delta\sigma})^{2/3} r^2 \quad (4)$$

N in (4), consistent with N in (1), is the number of earthquakes with dimension $\geq r$, and $\overline{\Delta\sigma}$ has been used for $\Delta\sigma$ in (3). It is empirically known that b is generally, but not always, very nearly equal to 1, irrespective of the choice of region and time interval in which earthquakes are counted. Also, c is empirically known to be 1.5 whether local magnitude M_L [Thatcher and Hanks, 1973] or surface wave magnitude M_s [Kanamori and Anderson, 1975] is used in (2), although serious departures from (2) with $c = 1.5$ begin to develop for $M_s \geq 7\frac{1}{2}$. Equation (4) implies that if the earthquakes of the counted sample share the same $\Delta\sigma$, as they do on the average for all samples for which the $\Delta\sigma$ have been determined [e.g., Hanks, 1977], earth-

quake magnitude frequency of occurrence statistics reduce to a simple matter of geometrical scaling in terms of the reciprocal faulting area.

Equation (1), however, is also satisfied (with a different a value) by the density distribution of the number of earthquakes with respect to M , $-dN/dM$ [Richter, 1958, p. 359]. In this interpretation the density distribution of the number of earthquakes with respect to r is proportional to r^{-3} , a result anticipated in the more complicated but essentially similar model of Caputo [1976].

To interpret (4), imagine a planar fault surface large in comparison to any earthquake source dimension of interest, and a population of incipient earthquakes to occur upon it; the earthquake population is characterized by the frequency of occurrence relation (4) and average stress drops equal to $\overline{\Delta\sigma}$ but with scatter about this value comparable to that observed in the available stress drop data. Before any of the earthquakes occur, all of the stress differences that will be realized at the time of occurrence for each and every event exist on the fault surface in 'potential' form; we denote this distribution in both spatial dimensions as the stress drop potential function $\Delta\sigma_p(x, y)$. As a matter of convenience, we assign zero mean to $\Delta\sigma_p(x, y)$ and denote the average shear stress on the fault as $\bar{\sigma}(y)$. In the earth, $\bar{\sigma}(y)$ is the average tectonic stress and is presumably a function of depth; it is not, however, sampled by earthquake stress drops or any other measure of the radiated field of earthquakes.

Within this framework we can expect the stress drop to be realized across an area of incipient rupture A to be derived from the root-mean-square (rms) value of $\Delta\sigma_p(x, y)$ over A , where we understand, purely as a formality, that only those regions of mostly positive $\Delta\sigma_p(x, y)$ are candidates for rupture. The mean-square value of $\Delta\sigma_p(x, y)$ across A is

$$\langle \Delta\sigma_p^2 \rangle = \frac{1}{A} \iint_A [\Delta\sigma_p(x, y)]^2 dx dy \quad (5)$$

Since $\Delta\sigma_p(x, y)$ produces earthquakes which, on the average, have stress drops $\sim \overline{\Delta\sigma}$ and satisfy the frequency of occurrence relation (4), (5) must be constant independent of A . Because of Rayleigh's theorem,

$$\frac{1}{A} \int_0^\infty [|\tilde{\Delta\sigma}_p(k)|]^2 k dk \quad (6)$$

must also be constant, independent of A , where $\tilde{\Delta\sigma}_p(k)$ is the two-dimensional Fourier transform of $\Delta\sigma_p(x, y)$ expressed in terms of radial wave number k ; wavelength λ is $2\pi/k$.

It is difficult to be general about the circumstances in which (6) will be constant for any A , but we can arrange a special case by assuming $|\tilde{\Delta\sigma}_p(k)| \sim k^{-n}$ and a band limitation for $\tilde{\Delta\sigma}_p(k)$ between k_{\min} and k_{\max} . Physically, the k^{-n} dependence of $|\tilde{\Delta\sigma}_p(k)|$ can be rationalized on the basis of similarity, and the band limitation means, for example, that λ greater than the seismogenic depth or less than a grain size do not contribute materially to $\Delta\sigma_p(x, y)$. Now, for $n > 1$ and $k_{\max} \gg k_{\min}$, the constancy of (6) requires that

$$A k_{\min}^{2n-3} = \text{const} \quad (7)$$

which, dimensionally, can only be arranged by taking $n = 2$ and $k_{\min} \sim A^{-1/2}$.

Physically, this means that the only significant spectral contributions to $\langle \Delta\sigma_p^2 \rangle$ occur at λ comparable to the source dimension of incipient rupture. For the k^{-2} dependence of $|\tilde{\Delta\sigma}_p(k)|$ it is, of course, clear that the shorter-wavelength contributions will be negligible, but for the same reason the

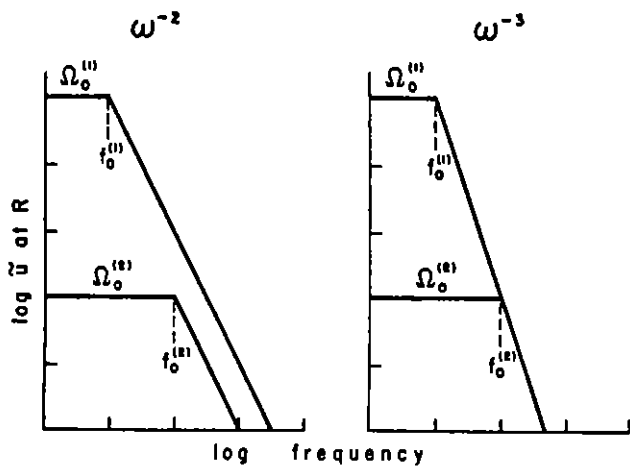


Fig. 1. Spectral representation of the ω^{-2} and ω^{-3} source models for two constant stress drop earthquakes observed at the same distance R in a uniform, elastic, isotropic full space.

longer λ contributions are plainly a problem. But if $\lambda \gg (A)^{1/2}$ made a significant contribution to $(\Delta\sigma_p^2)$ across our chosen A , then it is most likely that $(\Delta\sigma_p^2)$ across a larger A' would also be $\approx (\Delta\sigma)^2$; that is, in such an eventuality the rupture of A' would be the event of interest, having incorporated in its rupture the smaller area A . In other words, limiting the rupture area to some A must mean that $\lambda \gg A^{1/2}$ cannot contribute significantly to $(\Delta\sigma_p^2)$ across A ; otherwise, a larger area would rupture. As such, the frequency of occurrence relation (4) may be written as $N \sim (\lambda/\lambda_0)^{-2} \sim (k/k_0)^2$, where λ is the wavelength corresponding to any earthquake source dimension of interest and λ_0 is some reference source dimension.

In this context, then, a spectral composition of $\Delta\sigma_p(x, y)$ of the form $|\tilde{\Delta\sigma}_p(k)| \sim k^{-2}$ will guarantee constant stress drop earthquakes independent of the size of the rupture surface and that the frequency of occurrence relation will be satisfied. It is worth emphasizing, however, that this representation can well be nonunique and need not be correct, even though a different representation that will guarantee the constancy of (6) for any A is not obvious. We shall find, however, that the dynamic field radiated by earthquakes in the case of the $\gamma = 2$ model is consistent with $|\tilde{\Delta\sigma}_p(k)| \sim k^{-2}$ and provides separate support for this representation.

In supposing that these ideas are relevant to currently active crustal fault zones, some additional points should be made. First, stress drops both higher and lower than $\Delta\sigma$ will occur with certain probabilities determined by the distribution of $\Delta\sigma_p(x, y)$ about its rms value. Existing stress drop data are mostly in the range of several bars to several hundred bars, allowing for likely biasing to lower values in the case of many of the smaller earthquakes [Thatcher and Hanks, 1973; Hanks, 1977]. These determinations suggest a log normal distribution about a logarithmic mean of approximately 30 bars (Kanamori and Anderson [1975] have suggested $\Delta\sigma = 60$ bars on the basis of arithmetic averaging), one logarithmic standard deviation being about 0.5. Thus while the area-independent rms value of $\Delta\sigma_p(x, y)$ is determined by $\Delta\sigma \approx 30$ bars, it may vary, at least occasionally, to several hundred bars. It is interesting that this latter value is approximately the same as the variation about the mean of the frictional strength of common crustal rocks at constant pressure and temperature [Byerlee, 1978].

Second, active crustal fault zones are plainly not infinite in both spatial dimensions. For those earthquakes with fault length L sufficiently greater than fault width $w \approx h/\sin \delta$

(where h is the seismogenic depth and δ is the fault dip), the two-dimensional character of the fault surface collapses essentially to one, and it can be expected that the ideas presented above will no longer hold. For $h \approx 15$ km and a vertical transform fault, one may estimate roughly that this will occur when $L \geq 30$ km or, equivalently, when $M_s \geq 6\frac{1}{2}$. In particular, (3) then takes the form

$$M_0 = k' \Delta\sigma L w^2 \quad (8)$$

Moreover, (2) with $c = 1.5$ begins to fail at slightly larger M_s , 7–7 $\frac{1}{2}$. Finally, as is well known, M_s becomes an increasingly poorer measure of source strength for $M_0 \geq 10^{27}$ dyn cm, or $M_s \geq 7\frac{1}{2}$ [e.g., Kanamori, 1977]. As such, present uncertainties in estimating both c and 'magnitude' at large magnitude preclude, at the present time, an extension of these results to the more nearly one-dimensional character of large and great earthquakes. But these difficulties in no way change the arguments given above for $M_s \leq 6\frac{1}{2}$ earthquakes for which $r \leq w$.

EVIDENCE FOR AND INTERPRETATION OF THE ω^{-2} SOURCE MODEL

In spectral form the far-field radiation emanating from simple seismic source models [e.g., Aki, 1967; Brune, 1970, 1971] is generally characterized by a long-period level Ω_0 proportional to M_0 , a corner frequency f_0 proportional to r^{-1} , and a high-frequency spectral decay of the form $(f/f_0)^{-\gamma}$ (in the following discussion, frequency is denoted by f in hertz rather than ω in radians per second). The corner frequency f_0 , fundamentally, is closely allied with the reciprocal duration of faulting T_d^{-1} , but it is well known that several 'faulting durations' can be defined, in particular those associated with the fault length, fault width, and the rise time of a propagating displacement discontinuity. Depending on the faulting geometry and rise time characteristics, the associated corner frequencies can be well separated, leading to more complicated high-frequency spectral amplitude decay (that is, γ is a function of frequency). Moreover, by making the displacement discontinuity a smooth enough function of time, γ can become arbitrarily large at high enough frequencies. Whether in fact a generally applicable source representation of high-frequency spectral characteristics exists within the infinity of possibilities is as yet theoretically controversial and observationally unresolved. More as a matter of convenience than a matter of hard fact, high-frequency spectral characteristics of seismic sources are generally discussed in terms of Ω_0 and f_0 related by the constant stress drop assumption ($\Omega_0 f_0^2 = \text{const}$ in the context of the Ω_0 - f_0 relations of Hanks and Thatcher [1972]) and $\gamma = 2$ (the ω -square model) or $\gamma = 3$ (the ω -cube model, in the terminology of Aki [1967]).

Figure 1 schematically illustrates the $\gamma = 2$ and $\gamma = 3$ seismic source models in terms of two idealized far-field shear wave displacement spectral amplitudes at the same distance R . In both the $\gamma = 2$ and $\gamma = 3$ cases the two earthquakes have been assigned the same $\Delta\sigma$, so the corner frequencies lie on a line of slope -3 in these log-log plots. In both cases the larger event (event 1) has Ω_0 and M_0 3 orders of magnitude larger than the smaller event (event 2), and $f_0^{(1)}$ is 10 times smaller than $f_0^{(2)}$.

At frequencies greater than $f_0^{(2)}$, spectral amplitudes are 10 times greater for event 1 than for event 2 in the $\gamma = 2$ case but are the same in the $\gamma = 3$ models. How do we interpret these models in terms of time-domain amplitudes, recognizing that $T_d^{(1)} \approx 10T_d^{(2)}$? Figure 2 presents the extreme interpretations. Here, for purposes of illustration we have taken $f_0^{(1)} = 0.05$

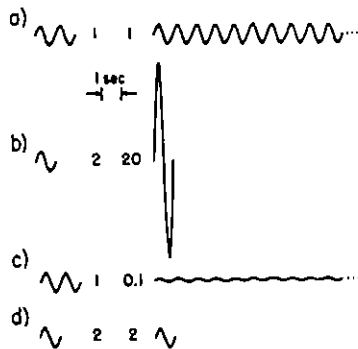


Fig. 2. Time domain interpretation of the ω^{-2} and ω^{-3} source models: (a) ω^{-2} model when 1-s radiation arrives continuously across T_d (2 s on the left-hand side and 20 s on the right-hand side, of which only 10 s are shown in the figure), (b) ω^{-2} model when 1-s radiation arrives in the first 1-s interval, (c) ω^{-3} model when 1-s radiation arrives continuously across T_d , and (d) ω^{-3} model when 1-s radiation arrives in the first 1-s interval. Relative 1-s amplitudes are given in two groups of four, one for the ω^{-2} model interpretation and one for the ω^{-3} model interpretation; the choice of 1 in the upper left-hand corner of each square is arbitrary.

Hz, $f_0^{(2)} = 0.5$ Hz, $T_d^{(1)} = 20$ sec, and $T_d^{(2)} = 2$ sec, and we are investigating possible interpretations of 1-s time domain amplitudes, those used in determining m_b .

Figure 2a is the interpretation for the $\gamma = 2$ earthquakes if the 1-s energy arrives more or less continuously over the complete faulting duration. In this case, 1-s spectral amplitudes for the larger event are 10 times greater than for the smaller event, but the 1-s time domain amplitudes are the same for both events—they have the same m_b . If all the 1-s energy arrives at the same time, however, the 1-s time domain amplitudes and m_b of the larger event are 10 times larger (Figure 2b).

For the $\gamma = 3$ earthquakes, 1-s spectral amplitudes must be the same. In Figure 2c this is achieved in a manner analogous to that in Figure 2a, but now 1-s time domain amplitudes for event 1 are 10 times smaller than for event 2; that is, m_b must decrease with M_0 . Figure 2d is the analogue to Figure 2b; here 1-s time domain amplitudes for the two earthquakes are the same; they have the same m_b .

The interpretation in Figure 2c is certainly unacceptable: m_b does not systematically decrease with increasing M_0 . Neither, however, does m_b increase beyond $m_b \approx 6\frac{1}{2}$ –7, and the interpretation in Figure 2b is also inappropriate, at least for $M_0 \geq 10^{26}$ dyn cm. One's preference for the interpretation in Figure 2a or 2d and thus one's preference for $\gamma = 2$ or $\gamma = 3$ seismic source models then depends on whether one believes that all (or most) of the 1-s energy arrives more or less continuously through T_d ($T_d > 1$ s) or arrives more or less impulsively in a ~ 1 -s window (and in the case of m_b , the first one or two such windows) no matter what the value of T_d . It is appropriate to recall now that both possibilities are extreme, and grossly simplified, interpretations; the truth, in most cases, should lie somewhere in between. Even so, when $T_d \gg 1$ s in the case of the larger earthquakes ($M_0 \approx 6\frac{1}{2}$), it is clear that Figure 2d is much more the exception than the rule, as almost all short-period seismograms of large and great earthquakes reveal. Thus I conclude, as Aki [1967] did more than a decade ago, that m_b - M_s data support the $\gamma = 2$ model, in the interpretation of Figure 2a, as the one generally (but certainly not always) applicable to the representation of high-frequency spectral characteristics.

With the assumptions that (1) fault propagation in both coordinates of the fault plane is equally phase coherent and (2) the source displacement time function is a propagating ramp

of finite duration (with singular particle accelerations), Geller [1976] followed Haskell [1964] to obtain $\gamma = 3$ at high frequencies. His justification of this model with existing m_b - M_s data is not correct, however, because he assumed that m_b and M_s faithfully represent spectral amplitudes at 1- and 20-s periods, respectively, across the entire range of magnitudes observable at teleseismic distances. Geller [1976] notes that 'it is not exactly correct' to do this; quite generally, it is not at all correct to do this, except for the smaller earthquakes ($M \geq 5$) for which $f_0 \geq 1$ Hz. In the latter case, both m_b and M_s become long-period measurements, proportional to M_0 , but then, of course, m_b - M_s data carry no information at all about high-frequency spectral characteristics of earthquake sources.

There are, in addition, several other observations that are in general accord with the high-frequency spectral characteristics of the ω^{-2} model. First, the difference of a factor of 20 in the maximum m_b of ~ 7.0 and maximum M_s of ~ 8.3 is 'exactly' predicted by the $\gamma = 2$ model (because of the period shift in the amplitude measurement from 1 to 20 s) provided that $m_b \approx M_s$ at ≈ 7 . In the 'latest' form of the linear relations between m_b and M_s , $m_b = M_s$ at 6.75 [Richter, 1958, p. 348]. Second, the same arguments used above to justify the $\gamma = 2$ model in terms of m_b and M_s data, and the upper limit to each, may also be used to explain why peak acceleration data at a fixed, close distance are such a weak function of magnitude, especially above $M_L \approx 4\frac{1}{2}$ –5 [Hanks and Johnson, 1976].

Third, the high-frequency spectral characteristics of the San Fernando earthquake are very well known [Berrill, 1975], even at frequencies 2 orders of magnitude greater than $f_0 = 0.1$ Hz [Wyss and Hanks, 1972], because of the large number of strong motion accelerograms that recorded this earthquake at local distances. With allowance for radiation pattern effects and anelastic attenuation, the $\gamma = 2$ model of Brune [1970, 1971], parameterized by $M_0 = 10^{26}$ dyn cm and $r = 10$ km, is the simplest possible interpretation of the data, although more complicated interpretations are possible and, in view of the highly inhomogeneous character of faulting for this earthquake, perhaps warranted.

Finally, a great number of spectral determinations have been made in the course of numerous source parameter studies, although the great bulk of these are single-station measurements (in addition to those cited by Hanks [1977], see also Trifunac [1972a, b], Johnson and McEvilly [1974], Bakun et al. [1976], and Hartzell and Brune [1977]). Of the three parameters Ω_0 , f_0 , and γ , γ is almost always the least well determined. Even so, $\gamma = 2$ is the value most often recovered, although the same observations clearly demonstrate that γ is not precisely 2, or even particularly close to it, for each and every earthquake. Still and all, the several sets of observations summarized in this section leave little alternative to the conclusion that the $\gamma = 2$ model is the one generally, if certainly not always, operative.

Figure 3 presents the acceleration spectral amplitudes, in the presence of anelastic attenuation for the two $\gamma = 2$ events whose displacement spectral amplitudes are given in Figure 1. In the frequency band $f_0 \leq f \leq f_{max}$, acceleration spectral amplitudes are constant, f_{max} being determined by setting the argument of the exponent in the expression $e^{-\pi f R / Q\beta}$ equal to 1. Then one interpretation, again nonunique, of Figure 3 is that the corresponding acceleration time histories are band-limited ($f_0 \leq f \leq f_{max}$), finite duration ($0 \leq t - R/\beta \leq T_d$) white noise. The whiteness arises from the constant spectral amplitudes equal to $\Omega_0 f_0^2$ in the band $f_0 \leq f \leq f_{max}$. The randomness has simply been assumed, but in view of the generally chaotic nature of strong motion accelerograms for

$M \sim 5$ earthquakes at $R \lesssim 10$ km, in finite time windows and frequency bands, this assumption does not seem unreasonable. Indeed, the idea that ground acceleration time histories can be treated as band-limited, finite duration white noise has been the basis for considerable work in the analysis of existing accelerograms and in the computation of synthetic accelerograms for more than 30 years in the engineering community [e.g., Housner, 1947; Hudson, 1956; Bycroft, 1960; Housner and Jennings, 1964; Jennings et al., 1968].

Hanks and Johnson [1976] developed the following relation between the amplitude \ddot{u} of any acceleration pulse at R and the dynamic stress difference σ_d giving rise to it in the source region:

$$\ddot{u} = \frac{1}{\rho} \frac{\sigma_d}{R} \quad (9)$$

where ρ is density. In this framework the interpretation of the $\gamma = 2$ model given above in terms of band-limited, finite duration white noise in ground acceleration translates directly into a white, random distribution of dynamic stress differences (at wavelengths less than r), but only with respect to the essentially one-dimensional configuration of Figure 3. That is, loosely speaking, the abscissa of Figure 3 is a one-dimensional wavelength spectrum of a two-dimensional faulting process. Now, if the radiated field is drawn from $|\tilde{\Delta\sigma}_p(k)| \sim (k/k_0)^{-2}$ and if the number of contributions to the spectral representation of the radiated field at frequency f , where $f \sim k$, is proportional to $(k/k_0)^2$, as suggested by the quasi-static frequency of occurrence relation (4), then the wave number spectrum of the radiated dynamic stress differences will be constant for $k \gtrsim 1/r$. Through (9) this implies a white acceleration spectrum and thus the $\gamma = 2$ model of the far-field shear displacement spectrum.

DISCUSSION

The consistency of the spectral composition inferred for $\Delta\sigma_p(x, y)$ and the $\gamma = 2$ model of the high-frequency radiated field is notable, in view of the grossly differing time and dimension scales associated with them individually (as long as several decades and hundreds of kilometers in the case of $\Delta\sigma_p(x, y)$ and as short as fractions of seconds and tens of meters in the case of the $\gamma = 2$ model for small earthquakes). Because of the variety of uncertainties and unknowns associated with this coincidence, it is probably premature to make too much of it or reach too far for its physical significance. Even so, it would follow quite naturally if the tectonic stress along active crustal fault zones was of the form $\bar{\sigma}(y) + \Delta\sigma_p(x, y)$, with the previously described characteristics for each.

If this is the case, b values different from 1 might be accompanied by γ different from 2 for those earthquakes of the

counted sample. In particular, when $b < 1$, there is a relative excess of larger earthquakes to smaller earthquakes, which may be interpreted in terms of $|\tilde{\Delta\sigma}_p(k)|$ deficient in short-wavelength amplitudes relative to a normative k^{-2} dependence; then $\gamma > 2$ would be expected if the dynamic stress differences arise from the same tectonic stress fields. Presently available data, unfortunately, are not suited for a critical examination of this hypothesis principally because of the poor control on γ .

Correlations of well-determined b -value and γ data may be particularly important to develop in view of the suggestion that b decreases prior to larger earthquakes and is therefore a possible means of earthquake prediction [Scholz et al., 1973; Wyss and Lee, 1973; Rikitake, 1975], although the data are hardly conclusive on this matter [Lahr and Pomeroy, 1970]. With respect to the ideas presented here, several points are worth making about this possibility. First, if $b = 1$ in a certain region over a long enough period of time, then b values estimated over a shorter period of time that explicitly excludes a larger earthquake (i.e., the one to be predicted) will be naturally biased to values that are greater than one, not less than one. Thus those areas with $b < 1$ in a time interval just before an earthquake larger than any member of the set counted to determine b are especially interesting. Second, as discussed previously, one interpretation of $b < 1$ is that $|\tilde{\Delta\sigma}_p(k)|$ is relatively deficient in short-wavelength amplitudes; the development of longer-wavelength stress concentrations would seem to be a natural prelude to the occurrence of a larger earthquake. Third, if $b < 1$ is accompanied by $\gamma > 2$ for those earthquakes that are counted to define b , one may proceed on an earthquake-by-earthquake basis rather than waiting the much longer period of time for enough earthquakes to yield a well-determined b . Another possibility, and an important one, is that b different from 1 may be accompanied by earthquake stress drops that are not independent of source size. More generally, if changes in any one of the normative situations of b values near 1, the general validity of the $\gamma = 2$ model, the constancy of earthquake stress drops independent of size, and $|\tilde{\Delta\sigma}_p(k)| \sim k^{-2}$ occur as a result of processes premonitory to larger-scale faulting, it seems reasonable that at least one and perhaps all of the other phenomena will change as well.

Finally, it is worth noting that if, as in the interpretation here, the frequency of occurrence statistics, or b values, are governed by the spectral composition of $\Delta\sigma_p(x, y)$, then the overall rate of seismicity, or a value, is presumably controlled by $\bar{\sigma}(y)$. At least along major plate margins, $\bar{\sigma}(y)$ increases slowly on a time scale of hundreds of years until the area of interest is ruptured by throughgoing faulting, at which time $\bar{\sigma}(y)$ precipitously decreases by the earthquake stress drop. It is well known that the San Francisco Bay area, to a considerable distance away from the San Andreas fault, was considerably more seismic at the $M \gtrsim 6$ level in the ~ 70 years prior to the 1906 earthquake than it has been in the ~ 70 years since [Tocher, 1959], excluding the immediate aftershock sequence, and it seems reasonable that a stress drop of approximately 100 bars along the San Andreas fault at the time of the earthquake played a central role in the greatly reduced seismicity rate. At the same time, however, this situation underscores the potential ambiguity at all wavelengths $\gtrsim h$ between the long-wavelength character of $\Delta\sigma_p(x, y)$ and $\bar{\sigma}(y)$ variable along the fault length.

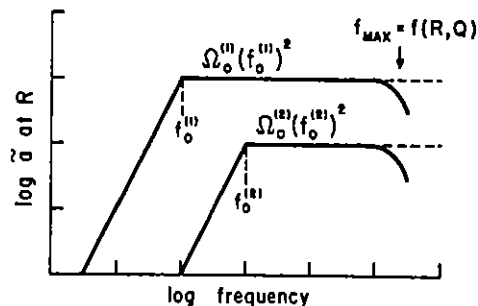


Fig. 3. Acceleration amplitude spectra at R for the ω^{-2} earthquakes of Figure 2, with attenuation explicitly shown.

HIGH-FREQUENCY STRONG GROUND MOTION

Whether or not b values and γ are related through a common origin in a tectonic stress of the form $\bar{\sigma}(y) + \Delta\sigma_p(x, y)$

along active crustal fault zones, as discussed in the last section, the general validity of the $\gamma = 2$ model has important implications for new approaches to the estimation of high-frequency strong ground motion for aseismic design purposes. One possibility that suggests itself immediately is developed below, in comparison with the existing approach. The alternate point of view, that strong motion accelerograms written at close distances ($R \approx 10$ km) for potentially damaging earthquakes are important data for investigating in more detail the validity of the $\gamma = 2$ model, shall be left as being implicit.

Since the first strong motion accelerograms were written more than 40 years ago, peak acceleration has been the most commonly used single index of strong ground motion. It has, however, been known for some time that peak acceleration need not be, and too often cannot be, a uniformly valid measure of strong ground motion over the entire frequency band and amplitude range of engineering interest. The very character of the peak acceleration datum as a short-period, time domain amplitude measurement is the principal reason for two important limitations on its value as a measure of strong ground motion. First, for $M \geq 5$ earthquakes at close distances, taken here as a rough threshold of potentially damaging ground motion, the period of this phase is much shorter than the faulting duration. Thus the peak acceleration simply cannot measure gross source properties of potentially damaging and destructive earthquakes, even if such data may, in a large enough set of observations, indicate limiting conditions on the failure process in very localized regions of the fault surface. Second, this same characteristic of the peak acceleration datum makes precise corrections for wave propagation effects, including anelastic attenuation and elastic scattering, impossible except under very unusual conditions. Both of these problems, but especially the second, are in turn responsible for the notoriously large scatter in peak acceleration data, even through very small variations of magnitude, distance, and site conditions. It is this last problem that limits the utility of peak acceleration even as a measure of high-frequency strong ground motion.

These difficulties in interpreting, manipulating, and extrapolating peak acceleration data are widely acknowledged by engineers and seismologists alike, and recently acquired peak acceleration data for $3 \leq M \leq 5$ earthquakes at $R \approx 10$ km have accentuated them [Hanks and Johnson, 1976; Seekins and Hanks, 1978]. But if peak acceleration is not a reliable measure of high-frequency strong ground motion, as is generally agreed to be the case, then what is?

One such measure that is almost certainly better is the rms acceleration, a_{rms} . First, since the time integral of the square ground acceleration is proportional to the work per unit mass done on a set of linear, viscously damped, single-degree-of-freedom oscillators with natural frequencies between 0 and ∞ [Arias, 1970], a_{rms} is then of considerable engineering importance (to the extent that actual structures may be approximated by such oscillators) with respect to the design capabilities of the rate of dissipation of this energy. Second, as a broadband integral measure, it almost certainly will be a more stable measure of high-frequency strong ground motion than individual high-frequency time domain amplitude measurements. Finally, as described below, a_{rms} can be directly related to a very few parameters of the earthquake source and source-station propagation path and thus can be estimated in the absence of strong ground motion observations or empirical correlations derived from them.

The analysis begins with Parseval's theorem,

$$\int_{-\infty}^{\infty} |a(t)|^2 dt = \frac{1}{2\pi} \int_{-\infty}^{\infty} |\tilde{a}(\omega)|^2 d\omega \quad (10)$$

where $a(t)$ is the acceleration time history and $\tilde{a}(\omega)$ is its Fourier amplitude spectrum. For $\tilde{a}(\omega)$ we take the $\gamma = 2$ model of Figure 3 and note that for large earthquakes at close distances, $f_{max} \gg f_0$, so that contributions to the right-hand side of (10) for $f \leq f_0$ are small. We further assume that the significant motion is confined to the shear wave arrival window $0 \leq t - R/\beta < T_d$ and anelastic attenuation cuts the spectral amplitudes off sharply at $f \approx f_{max}$. Then (10) may be written

$$\int_0^{T_d} |a(t)|^2 dt = \frac{2}{2\pi} \int_{2\pi f_0}^{2\pi f_{max}} |\tilde{a}(\omega)|^2 d\omega \quad (11)$$

The rms acceleration is

$$a_{rms} = \left[\frac{1}{T_d} \int_0^{T_d} |a(t)|^2 dt \right]^{1/2} \quad (12)$$

Equations (11) and (12), together with

$$\tilde{a}(\omega) = \Omega_0 (2\pi f_0)^2 \quad f_0 \leq f \leq f_{max} \quad (13)$$

and the approximation

$$f_0 = 1/T_d \quad (14)$$

result in

$$a_{rms} = 2^{1/2} (2\pi)^2 \Omega_0 f_0^2 (f_{max}/f_0)^{1/2} \quad (15)$$

for $f_{max} \gg f_0$. Finally, for the Brune [1970, 1971] scaling,

$$\Delta\sigma = 106\rho R \Omega_0 f_0^3 \quad (16)$$

[Hanks and Thatcher, 1972], which, upon substitution in (15), gives

$$a_{rms} = 0.85 \frac{2^{1/2} (2\pi)^2}{106} \frac{\Delta\sigma}{\rho R} \left(\frac{f_{max}}{f_0} \right)^{1/2} \quad (17)$$

The factor of 0.85 introduced in (17) accounts for free surface amplification of SH waves (2.0), vectorial partition onto two horizontal components of equal amplitude ($1/2^{1/2}$), and the rms value of the shear wave radiation pattern (0.6) [Thatcher and Hanks, 1973].

Table 1 compares a_{rms} values estimated from (17) with observed, whole record values for the San Fernando earthquake at Pacoima Dam and the Kern County earthquake at Taft and with 'observed' values corrected for (record length/ T_d)^{1/2} to estimate the a_{rms} value that occurs in the time interval of the S wave arrival plus T_d . For the San Fernando earthquake the 'observed' value is 70% greater than the estimated value at Pacoima Dam; in the case of the Kern County earthquake at Taft the 'observed' value is only 30% greater than the estimated value. By conventional seismological standards in estimating high-frequency amplitudes, this agreement is remarkable.

These comparisons are, on the one hand, encouraging with respect to the use of a_{rms} as a measure of high-frequency strong ground motion and, on the other hand, further evidence for the general validity of the $\gamma = 2$ model. In both respects, however, further examination of existing data is required, and strong motion accelerograms at $R \leq 10$ km are a particularly valuable set of observations for these analyses.

TABLE 1. Comparisons of Estimated and 'Observed' a_{rms} Values

	San Fernando Earthquake at Pacoima Dam	Kern County Earthquake at Taft
$\Delta\sigma$, bars	50*	60*
f_0 , Hz	0.1†	0.05‡
R , km	~10	~40
f_{max} , Hz	~30§	~8§
a_{rms} , cm/s ²		
Estimated	140	30
Observed	120,110	26,27
'Observed'	240	39

*Kanamori and Anderson [1975].

†Hanks and Wyss [1972].

‡Estimated for $L = 50$ km, $r = L/2$, and $f_0 = 2.34\beta/2\pi r$.

§From $\pi f_{max} R/Q\beta = 1$ with $\beta = 3.2$ km/s and $Q = 300$.

||For both horizontal components, from Brady et al. [1971] for Pacoima Dam and Hudson and Brady [1969] for Taft.

SUMMARY AND CONCLUSIONS

The nature and magnitude of variations in the deviatoric stresses existing along active crustal fault zones are central to a full understanding of the cause and effect of earthquakes, but these variations are at the present time only poorly understood. These stresses may be written in the form $\bar{\sigma}(y) + \Delta\sigma_p(x, y)$, where $\bar{\sigma}(y)$ is the average tectonic stress at depth y and $\Delta\sigma_p(x, y)$ is the seismologically observable stress drop potential function. The constancy of earthquake stress drops independent of source dimension suggests that the spectral composition of $\Delta\sigma_p(x, y)$ is of the form $|\tilde{\Delta\sigma}_p(k)| \sim k^{-2}$. Independent support for this representation exists in the general validity of the $\gamma = 2$ model of the far-field shear wave displacement spectrum, under the reasonable assumptions that the radiated field of earthquakes is also drawn from the stress differences of $\Delta\sigma_p(x, y)$ and that the number of contributions to the radiated field at frequency f goes as $(k/k_0)^2$, consistent with the quasi-static frequency of occurrence relation $N \sim 1/r^2$. Separately, a variety of seismologic observations suggests that the $\gamma = 2$ model is the one generally, although certainly not always, applicable to the high-frequency spectral decay of the far-field radiation of earthquakes.

That the constancy of earthquake stress drops, b values near 1, and the general validity of the $\gamma = 2$ model may all be related to the same spectral composition of $\Delta\sigma_p(x, y)$ is a notable result, although there is as yet considerable uncertainty, especially in an observational sense, in relating these phenomena to a common physical origin, namely, $|\tilde{\Delta\sigma}_p(k)| \sim k^{-2}$. If, however, these phenomena indeed share a common explanation in a tectonic stress of $\bar{\sigma}(y) + \Delta\sigma_p(x, y)$ existing along active crustal fault zones, where $\Delta\sigma_p(x, y)$ has spectral composition $|\tilde{\Delta\sigma}_p(k)| \sim k^{-2}$, a possible consequence is that b values different from 1 would be accompanied by γ different from 2 for those earthquakes counted to determine b . Another is that changes in b values from 1 may be accompanied by earthquake stress drops different from $\Delta\bar{\sigma}$ and/or different from the normative area independence.

Irrespective of these possible associations, the $\gamma = 2$ model in the presence of anelastic attenuation suggests that high-frequency strong ground motion has a straightforward interpretation as band-limited, finite duration white noise in acceleration. An estimate of a_{rms} is easily constructed from this interpretation, and for several reasons it appears to be of potential importance as a measure of high-frequency strong

ground motion for aseismic design purposes. Alternatively, these same ideas, together with strong motion accelerograms written at close distances for potentially damaging earthquakes, may be used for investigating in more detail the $\gamma = 2$ model.

Acknowledgments. I have enjoyed the critical remarks of D. J. Andrews, A. McGarr, and W. Thatcher in developing the ideas of this manuscript and useful conversations with M. Caputo regarding frequency of occurrence statistics. I deeply appreciate the efforts of E. A. Flinn in his capacity of editor and an unknown associate editor in having me evaluate critically an original, and erroneous, guess that the spectral composition of $\Delta\sigma_p(x, y)$ was white, a guess written into the work of Hanks (1977) without consequence. Carol Sullivan patiently typed this manuscript several times. This research was supported in part by National Science Foundation grant ENV76-81816. Publication approved by the Director, U.S. Geological Survey.

REFERENCES

- Aki, K., Scaling law of seismic spectrum, *J. Geophys. Res.*, **72**, 1212-1231, 1967.
- Aki, K., Earthquake mechanism, *Tectonophysics*, **13**, 423-446, 1972.
- Andrews, D. J., Coupling of energy between tectonic processes and earthquakes, *J. Geophys. Res.*, **83**, 2259-2264, 1978.
- Arias, A., A measure of earthquake intensity, in *Seismic Design for Nuclear Power Plants*, edited by R. J. Hanson, MIT Press, Cambridge, Mass., 1970.
- Bakun, W. H., C. G. Bufe, and R. M. Stewart, Body-wave spectra of central California earthquakes, *Bull. Seismol. Soc. Amer.*, **66**, 363-384, 1976.
- Berrill, J. B., A study of high-frequency strong ground motion from the San Fernando earthquake, Ph.D. thesis, Calif. Inst. of Technol., Pasadena, 1975.
- Bouchon, M., A dynamic source model for the San Fernando earthquake, *Bull. Seismol. Soc. Amer.*, **68**, 1555-1576, 1978.
- Brady, A. G., D. E. Hudson, and M. J. Trifunac, *Earthquake Accelerograms*, vol. 1, part C, Earthquake Engineering Research Laboratory, California Institute of Technology, Pasadena, 1971.
- Brune, J. N., Tectonic stress and the spectra of seismic shear waves, *J. Geophys. Res.*, **75**, 4997-5009, 1970.
- Brune, J. N., Correction, *J. Geophys. Res.*, **76**, 5002, 1971.
- Burdick, L. J., and G. R. Mellman, Inversion of the body waves from the Borrego Mountain earthquake to the source mechanism, *Bull. Seismol. Soc. Amer.*, **66**, 1485-1499, 1976.
- Bycroft, G. N., White noise representation of earthquakes, *J. Eng. Mech. Div. Amer. Soc. Civil Eng.*, **86**, 1-16, 1960.
- Byerlee, J., Friction of rocks, *Pure Appl. Geophys.*, **116**, 615-626, 1978.
- Caputo, M., Model and observed seismicity represented in a two-dimensional space, *Ann. Geofis.*, **29**, 277-288, 1976.
- Das, S., and K. Aki, Fault plane with barriers: A versatile earthquake model, *J. Geophys. Res.*, **82**, 5658-5670, 1977.
- Geller, R. J., Scaling relations for earthquake source parameters and magnitudes, *Bull. Seismol. Soc. Amer.*, **66**, 1501-1523, 1976.
- Hanks, T. C., The faulting mechanism of the San Fernando earthquake, *J. Geophys. Res.*, **79**, 1215-1229, 1974.
- Hanks, T. C., Earthquake stress drops, ambient tectonic stresses, and stresses that drive plate motions, *Pure Appl. Geophys.*, **115**, 441-458, 1977.
- Hanks, T. C., and D. A. Johnson, Geophysical assessment of peak accelerations, *Bull. Seismol. Soc. Amer.*, **66**, 959-968, 1976.
- Hanks, T. C., and W. R. Thatcher, A graphical representation of seismic source parameters, *J. Geophys. Res.*, **77**, 4393-4405, 1972.
- Hartzell, S. H., and J. N. Brune, Source parameters for the January 1975 Brawley-Imperial Valley earthquake swarm, *Pure Appl. Geophys.*, **115**, 333-355, 1977.
- Haskell, N. A., Total energy and energy spectral density of elastic wave radiation from propagating faults, *Bull. Seismol. Soc. Amer.*, **54**, 1811-1841, 1964.
- Heaton, T. H., and D. V. Helmberger, A study of the strong ground motion of the Borrego Mountain, California, earthquake, *Bull. Seismol. Soc. Amer.*, **67**, 315-330, 1977.
- Housner, G. W., Characteristics of strong-motion earthquakes, *Bull. Seismol. Soc. Amer.*, **37**, 19-31, 1947.
- Housner, G. W., and P. C. Jennings, Generation of artificial earthquakes, *J. Eng. Mech. Div. Amer. Soc. Civil Eng.*, **90**, 113-150, 1964.
- Hudson, D. E., Response spectrum techniques in engineering seis-

- mology, in *World Conference on Earthquake Engineering*, Earthquake Engineering Research Institute, Berkeley, Calif. 1956.
- Hudson, D. E., and A. G. Brady, *Strong Motion Earthquake Accelerograms*, vol. 2, part A, Earthquake Engineering Research Laboratory, California Institute of Technology, Pasadena. 1969.
- Jennings, P. C., G. W. Housner, and N. C. Tsai, *Simulated Earthquake Motions*, Earthquake Engineering Research Laboratory, California Institute of Technology, Pasadena, Calif., 1968.
- Johnson, L. R., and T. V. McEvilly, Near-field observations and source parameters of central California earthquakes, *Bull. Seismol. Soc. Amer.*, *64*, 1855-1886, 1974.
- Kanamori, H., The energy release in great earthquakes, *J. Geophys. Res.*, *82*, 2981-2987, 1977.
- Kanamori, H., and D. L. Anderson, Theoretical basis of some empirical relations in seismology, *Bull. Seismol. Soc. Amer.*, *65*, 1073-1096, 1975.
- Lahr, J., and P. W. Pomeroy, The foreshock-aftershock sequence of the March 20, 1966 earthquake in the Republic of Congo, *Bull. Seismol. Soc. Amer.*, *60*, 1245-1258, 1970.
- Richter, C. F., *Elementary Seismology*, 768 pp., W. H. Freeman, San Francisco, Calif., 1958.
- Rikitake, T., Earthquake precursors, *Bull. Seismol. Soc. Amer.*, *65*, 1133-1162, 1975.
- Scholz, C. H., L. R. Sykes, and Y. P. Aggarwal, Earthquake prediction: A physical basis, *Science*, *181*, 803-810, 1973.
- Seekins, L. C., and T. C. Hanks, Strong motion accelerograms of the Oroville aftershocks and peak acceleration data, *Bull. Seismol. Soc. Amer.*, *68*, 677-689, 1978.
- Thatcher, W., and T. C. Hanks, Source parameters of southern California earthquakes, *J. Geophys. Res.*, *78*, 8547-8576, 1973.
- Tocher, D., Seismic history of the San Francisco region, San Francisco Earthquakes of March 1957, *Calif. Div. Mines Geol. Spec. Rep.*, *57*, 1959.
- Trifunac, M. D., Stress estimates for the San Fernando earthquake of February 9, 1971: Main event and thirteen aftershocks, *Bull. Seismol. Soc. Amer.*, *62*, 721-750, 1972a.
- Trifunac, M. D., Tectonic stress and the source mechanism of the Imperial Valley, California, earthquake of 1940, *Bull. Seismol. Soc. Amer.*, *62*, 1283-1302, 1972b.
- Wyss, M., and T. C. Hanks, The source parameters of the San Fernando earthquake inferred from teleseismic body waves, *Bull. Seismol. Soc. Amer.*, *62*, 591-602, 1972.
- Wyss, M., and W. H. K. Lee, Time variations of the average earthquake magnitude in central California, in *Proceedings of the Conference on Tectonic Problems of the San Andreas Fault System*, Stanford University Publications, Stanford, Calif., 1973.

(Received May 4, 1978;
revised November 3, 1978;
accepted January 1, 1979.)